HHS Public Access

Author manuscript

J Immunol. Author manuscript; available in PMC 2022 December 01.

Published in final edited form as:

J Immunol. 2021 December 01; 207(11): 2688–2698. doi:10.4049/jimmunol.2100218.

FCRL1 regulates BCR-induced ERK activation through GRB2

Jenna M. DeLuca[*], **Maegan K. Murphy**[*], **Xin Wang**[*], **Timothy J. Wilson**[*,2]

[*]Department of Microbiology, Miami University, Oxford, OH 45056, United States

Abstract

Regulation of B cell receptor signaling has important consequences for generating effective antibody responses to pathogens and preventing production of autoreactive B cells during development. Currently defined functions of FCRL1 include positive regulation of BCR-induced calcium flux, proliferation, and antibody production, however, the mechanistic basis of FCRL1 signaling and its contributions to B cell development remain undefined. Molecular characterization of FCRL1 signaling shows phosphotyrosine-dependent associations with GRB2, GRAP, SHIP-1, and SOS1, all of which can profoundly influence MAP kinase signaling. In contrast with previous characterizations of FCRL1 as a strictly activating receptor, we discover a role for FCRL1 in suppressing ERK activation under homeostatic and BCR-stimulated conditions in a GRB2-dependent manner. Our analysis of B cells in *Fcrl1*−/− mice shows that ERK suppression by FCRL1 is associated with a restriction in the number of cells surviving splenic maturation in vivo. The capacity of FCRL1 to modulate ERK activation presents a potential for FCRL1 to be a regulator of peripheral B cell tolerance, homeostasis, and activation.

Introduction

B cell development and activation are tightly regulated by the B cell receptor (BCR) signaling pathway. In the course of clonal selection and the immune response, the establishment of a threshold for B cell activation is critical for shaping an antibody repertoire with minimal auto-reactivity and high affinity for foreign antigens (1–6). In order to set a threshold appropriate for key developmental checkpoints, the outcome of the signal transduced by the BCR must be appropriate for the maturation state of the cell (7–10). One of the principal means by which this is accomplished is the differential expression of receptors that promote activation and survival signals. For example, tonic signals through the BCR are required for development, but may lead to apoptosis in transitional B cells unless coupled to a survival signal through BAFF-R (11–13). This constitutive modulation of the signals through the BCR promotes favorable biological outcomes by limiting the production

[2]**Correspondence:** Timothy J. Wilson, tim.wilson@miamioh.edu, Phone: (513) 529-1694, Fax: (513) 529-2431.

Author Contributions

Conceptualization, T.J.W, J.M.D, and M.KM; Methodology, T.J.W, J.M.D, X.W. and M.KM; Validation, J.M.D and M.K.M; Formal Analysis J.M.D and M.K.M; Investigation J.M.D, M.K.M, and X.W.; Resources, T.J.W. and X.W.; Data Curation, T.J.W. and J.MD.; Writing – Original Draft J.M.D, M.K.M, X.W., and T.J.W.; Writing- Review & Editing, T.J.W, J.M.D and M.K.M; Visualization, J.M.D and M.K.M; Supervision, T.J.W and J.M.D; Project Administration, T.J.W.; Funding Acquisition, T.J.W., J.M.D. and M.K.M.

Conflict of Interest

The authors declare no competing financial interests.

of autoreactive B cells while maintaining a pool of cells with signaling-competent BCRs (14).

The classical BCR signaling pathway is initiated by the cross-linking of BCR complexes, inducing the aggregation of CD79a and CD79b signaling chains. Immunoreceptor tyrosine-based activation motifs (ITAMs) of CD79a/b become phosphorylated by the Src family kinases FYN, LYN, and BLK and recruit spleen tyrosine kinase (SYK) (15, 16). SYK substrates include BLNK, BCAP, and CD19, allowing the recruitment of phosphoinositol-3-kinase (PI3K) to the BCR signaling complex for further downstream signaling through generation of IP_3 and DAG by PLCγ (14, 17–19). Downstream of IP_3 and DAG generation, the MAP kinase, NFAT, and NF-κB pathways may drive apoptosis, survival, development, proliferation, or differentiation, depending on the integration of signals by the cell (20, 21).

The differential consequences of BCR signaling on the fate of a B cell at specific maturation stages depend on the establishment of an activation threshold appropriate for the developmental status of the cell (21, 22). This threshold is partly determined by the balance of inhibitory and activating signals that modulate the response to antigen receptor engagement. While ITAMs drive recruitment of tyrosine and lipid kinases to promote activation, inhibitory receptors may signal through immunoreceptor tyrosine-based inhibitory motifs (ITIMs) to recruit inhibitory molecules including the protein tyrosine phosphatases SHP-1 and SHP-2 or the inositol phosphatases SHIP-1 and SHIP-2 (23, 24). In some cases, ITAM sequences are capable of recruiting these inhibitory effectors following a sustained activating signal (25, 26).

Among the activating and inhibitory receptors contributing to establishing the activation threshold for B cells are the Fc receptors (FcRs) FcεRII and FcγRIIb, along with the Fc receptor-like (FCRL) proteins. (27, 28). In both FcRs and FCRLs, immunomodulatory signals are transduced through phosphorylated tyrosines that are present in the cytoplasmic domain of either the receptor itself or a transmembrane adapter with which it pairs (25, 26, 29). Eight human and six mouse FCRL genes have been identified in leukocyte populations. Of the FCRL molecules, FCRL1–6 in humans and FCRL1 and FCRL5 in mice contain immunoreceptor tyrosine-based signaling motifs. Human FCRL2 and FCRL6 have been demonstrated to play a strictly inhibitory role in lymphocyte signal transduction, containing consensus ITIMs and recruiting SHP and SHIP phosphatases (30–33). FCRL3, FCRL4, and FCRL5 are all immunoglobulin receptors and appear to fulfill both activating and inhibitory functions in different contexts (34–43).

FCRL1 was first identified as an activating receptor capable of enhancing signaling through the B cell receptor. Human FCRL1 consists of three Ig-like domains and two ITAM-like sequences in its cytoplasmic tail. Mouse FCRL1 lacks the N-terminal Ig-like domain of the human ortholog, but retains multiple cytosolic tyrosines including an ITAM-like sequence (44). Although ligands for FCRL1 remain unknown, the presence of a putative ITAM sequence in its cytoplasmic tail suggests a role in B cell activation. *Fcrl1*$^{-/-}$ mice have been observed to exhibit impaired antibody responses to both thymus-dependent and independent antigens, diminished activated B cells following immunization, and impaired BCR signalosome formation (45). In both human and mouse B cells, FCRL1 positively

regulates B cell proliferation and calcium mobilization (44–46). Knockdown of FCRL1 in human B cell lymphomas is associated with increased apoptosis, explained by the downregulation of the anti-apoptotic *Bcl2* gene and upregulation of the pro-apoptotic *Bid* and *Bax* genes (46). While these results strongly suggested an activating role for FCRL1 in B cell signal transduction, the molecular mechanism by which FCRL1 regulates B cell activation remains to be fully defined. Moreover, FCRL1 expression varies in different subsets of human B cells (44). Although this suggests a role for FCRL1 in B cell selection and maturation, its significance in B cell development remains to be investigated. Using biochemical techniques and *Fcrl1*$^{-/-}$ mice, we observe a role for FCRL1 in regulating B cell numbers during development linked to an unexpected role for FCRL1 in negatively regulating ERK activation downstream of BCR engagement through interactions of FCRL1 with GRB2.

Materials and Methods

Mice

Fcrl1$^{-/-}$ (B6;129S5-*Fcrl1*^{tm1Lex}/Mmucd; RRID: MMRRC_032301-UCD) mice were from the Mutant Mouse Resource and Research Center: UC Davis (MMRRC). WT 129S1/SvImJ to which *Fcrl1*$^{-/-}$ mice were backcrossed for at least five generations were from The Jackson Laboratory. Backcrossing was confirmed by simple sequence length polymorphism (SSLP) genotyping to select breeders on the 129/SvImJ background. Mice were group housed in pathogen-free conditions and under a standard diet. All functional experiments were conducted in age and sex matched cohorts of *Fcrl1−/−* and WT mice eight to twelve weeks of age. Analyses of B cell development and FCRL1 expression patterns were replicated in both male and female cohorts. All animal experiments were approved by the Miami University Institutional Animal Care and Use Committee.

Generation of FCRL1-specific monoclonal antibodies

FCRL1 peptide (aa 319–343) coupled to keyhole limpet hemocyanin (KLH-CSFQVSSGLYSKPRINIAHMDYEDAM) was purchased from Biomatik (Ontario, Canada). Monoclonal anti-mouse FCRL1 (350G10) was generated by immunizing 129/SvImJ mice twice by intraperitoneal injection with FCRL1-KLH precipitated in alum, and a final immunization in the absence of adjuvant. Three days after the final immunization, splenocytes were fused with SP2/0 mouse myeloma cell line and placed under hypoxanthine-aminopterin-thymidine selection. Supernatants from 459 of the resulting clones were screened for reactivity first by enzyme-linked immunosorbent assay (ELISA) and by western blotting on immortal and primary cells. Of these, 14 clones were found to recognize mouse FCRL1 in splenocytes and immortal cells but not knockout controls. Clone 350G10 (IgG2b) was expanded for purification and characterization.

Cell Lines

A20IIA1.6 cells were a gift from John Cambier (Department of Immunology & Microbiology, University of Colorado - Denver). A20IIA1.6 and HEK293T (ATCC CRL-3216) cells were cultured at 37°C and 5% CO_2 in RPMI supplemented with 5%

FCS, 100 units/mL penicillin/streptomycin, 1 mM sodium pyruvate, 1mM Glutamax, and 0.00025% 2-mercaptoethanol.

Construct and Cell Line Generation

CRISPR Knockout Cell Lines.—For CRISPR plasmid generation, pLentiCRISPRv2Δ*Fcrl1* targeting the sequence 5'-GCCTGGTCCTCATGCTACCT-3' was custom-ordered (GenScript), and annealing oligos targeting the sequence 5'-CTTCCCGGCTCCGTCG-3' of GRB2 were ligated into the *BsmBI*-digested pLentiCRISPRv2 to generate pLeniCRISPRv2Δ*Grb2*. 293T cells were transfected for 72 hours with lentiviral expression vector together with pMDG.2 and pSPAX2 (Gift from Didier Trono, Addgene: 12260 and 12259) packaging vectors in polyethyleneimine prior to transduction of A20IIA1.6 cells. Viral supernatants were collected, filtered with 1.2 μM pore syringe filters, and transferred to A20IIA1.6 cells. Cells underwent 72 hours of transduction followed by a week of selection in 3μg/mL puromycin. FCRL1 knockout cells were stained for endogenous FCRL1 (REA566, Miltenyi Biotec) and sorted for ablated FCRL1 expression using a FACSMelody cell sorter (BD Biosciences). *Grb2* knockout cells underwent single cell sorting, and individual clones were screened by immunoblotting.

FCRL1 Mutant and Overexpression Cell Lines.—A codon-optimized, N-terminal FLAG-tagged FCRL1 cDNA sequence containing an internal *BamHI* restriction site and a 3' *SalI* restriction site for further mutagenesis was custom-ordered from Genscript. The insert sequence was ligated into pLenti-CMV-GFP-Puro vector (Gift from Eric Campeau, Addgene: 17448), replacing the eGFP with *Fcrl1*. For the generation of $Y_{281}F$ and $Y_{297}F$ mutants, PCR site-directed mutagenesis was conducted on the WT FCRL1 template, and the *BamHI*- and *SalI*- digested amplicons were cloned into the WT vector. For the generation of the 6YF mutant, a custom-ordered 5YF oligonucleotide sequence encoding mutations $Y_{281}F$, $Y_{293}F$, $Y_{297}F$, $Y_{327}F$, and $Y_{339}F$ was digested with *BamHI* and *SalI* and ligated into the WT vector. Subsequently, PCR-based site directed mutagenesis from the 5YF template was used to generate the $Y_{268}F$ mutation. All constructs were sequence-verified prior to use. Because FCRL1 overexpression constructs would be expressed in puromycin-selected FCRL1 or GRB2 deficient cell lines, a neomycin-resistance gene from pLenti-CMV-GFP-Neo vector was substituted for the puromycin resistance gene in pLenti-CMV-Puro by digestion with *SalI* and *NheI.* FCRL1- or GRB2-deficient A20IIA1.6 cells were transduced as previously described and subjected to selection in 1mg/mL G418 prior to staining for FLAG expression (L5, BioLegend) and sorting with a BD FACSMelody cell sorter. For the generation of the GRB2 fusion construct with the C-terminus of FCRL1–6YF, stitching PCRs were performed followed by ligation into the 6YF vector described above.

Immunoprecipitations

Transduced A20 IIA1.6 cells (100–250 million for mass spectrometry, 30 million for western blotting) were incubated at 37°C for 15 minutes in un-supplemented RPMI with 0.5 mM pervanadate or for 5 minutes with 10μg/ml goat F(ab')2 anti-mouse Ig (H+L) (Southern Biotech). Cells were lysed in PBS containing 1% Triton X-100 (v/v), 1 mM EDTA, 1mM orthovanadate, and 1x SIGMAFAST Protease Inhibitor Cocktail (Sigma-Aldrich). Lysates were immunoprecipitated, rotating, for 2 hours at 4°C with antibody-

bound beads. For immunoprecipitations followed by western blotting, 3 μg biotinylated anti-FLAG L5 (BioLegend) or biotinylated anti-FCRL1 (Miltenyi Biotec), were pre-incubated with an appropriate volume of streptavidin magnetic beads (New England Biolabs). For immunoprecipitations followed by mass spectrometry, 25μg biotinylated anti-FLAG were pre-incubated one hour at 4°C with appropriate volumes of streptavidin-conjugated T1, C1, or M-280 Dynabeads (ThermoFisher Scientific). Beads were washed twice in PBS prior to antibody incubation and were washed once in lysis buffer after antibody incubation. Lysates were incubated with the beads for 2 hours at 4°C with rotation. Immunoprecipitated samples were washed three times in lysis buffer at 4°C. Samples were eluted for 10 minutes at 55°C in SDS loading dye for western blotting or for 20 minutes at 60°C in Cell Lysis Buffer from the Pierce Mass Spec Sample Prep Kit for Cultured Cells (Thermo Scientific) for mass spectrometry.

Western Blotting

Samples in SDS loading dye were reduced by heating at 95°C with 2-mercaptoethanol. Samples were loaded on a Bolt 4–12% Bis-Tris Plus gel (Invitrogen), electrophoresed in MOPS running buffer, transferred to a PVDF membrane, and immunoblotted. Immunoblots were probed with 0.1 μg/mL mouse anti-phosphotyrosine PY20 (Southern Biotech), 0.5 μg/mL anti-SHIP1 (Invitrogen), 0.5 μg/mL anti-GRB2 (Cell Signaling Technologies),1 μg/mL anti-SOS1 (Cell Signaling Technologies), 0.5 μg/mL anti-FLAG L5 (BioLegend), or 0.5 μg/mL anti- FCRL1 350G10 which was generated in our lab. Secondary antibodies including 0.5 μg/mL anti-rat IgG (Cell Signaling Technologies, Danvers, MA, USA), 0.5 μg/mL anti-rabbit IgG (Cell Signaling Technologies), or 0.1 μg/mL anti-mouse IgG2b (Southern Biotech) were used according to the isotype and host species of primary antibody. Blocking and diluted antibody solutions consisted of 1% BSA in HEPES-buffered saline with 1 mM EDTA and 0.1% TWEEN-20. Blots were developed using SuperSignal West Pico PLUS Chemiluminescent Substrate (Thermo Scientific) and imaged using a ChemiDoc gel imager (Bio-Rad).

Mass Spectrometry

Immunoprecipitated A20IIA1.6 parent cells, WT, and 6YF samples were eluted at 60°C for 20 minutes in Cell Lysis Buffer from the Pierce Mass Spec Sample Prep Kit for Cultured Cells (Thermo Scientific). Protein concentration was quantitated by NanoDrop and adjusted to 100μg for reduction, alkylation, acetone precipitation, Lys-C digestion, and trypsin digestion according to the manufacturer's protocol. 30μg of peptides from each sample, as determined by NanoDrop, were purified with Pierce C-18 Spin Columns according to the manufacturer's protocol (Thermo Scientific). Samples were speed vacuumed, resuspended in 0.1% formic acid, and centrifuged to pellet debris. Two μg of the digested peptides were analyzed by loading onto a C18 capillary column coupled to the Thermo LTQ XL Orbitrap Mass Spectrometer at the Miami University Mass Spectrometry Facility. The peptides were scanned at the mass range of 350–1800 mass-to-charge ratio with the resolution of 30,000. Peptide identities were analyzed using the program Patternlab for Proteomics (47), with the mass increase of 79.9663 added to the search parameter to identify potential phosphorylation modifications to tyrosine.

Flow Cytometry

B Cell Population Panels: Spleens and bone marrow (BM) from naïve mice were harvested from age- and sex-matched cohorts, and red blood cells were lysed by ammonium chloride lysis. Splenocytes were incubated for 30 minutes on ice with the following antibodies and dyes: viability (Zombie Aqua, Biolegend), anti-B220 (RA3–6B2, BD Biosciences), anti-CD19 (6D5, Biolegend), anti-CD23 (B3B4, Biolegend), anti-CD93 (AA4.1, Biolegend), anti-Ly77 (GL7, Biolegend), anti-IgD (11-26C.2a, Biolegend), anti-IgM (RMM1, Biolegend). and anti-F4/80 (BM8, Biolegend). BM was incubated for 30 minutes on ice with the following antibodies and dyes: anti-B220 (RA3–6B2, BD Biosciences), anti-CD138 (281-2, Biolegend), anti-VpreB (R3, Biolegend), and anti-CD24 (M1/69, Biolegend). FCRL1 expression in different cell types in the bone marrow and spleen was tracked with anti-CD307a (REA566, Miltenyi).

Proliferation assays.—To track proliferation in vivo, mice were injected with 1 mg BrdU and 24 hours later, spleens were harvested and processed according to manufacturer's instructions for the BD Biosciences BrdU Flow Kit (559619, BD Biosciences). Samples were analyzed on an LSRII Flow Cytometer (BD Biosciences). Cell cycle analysis of bone marrow and splenic B cells were performed by staining leukocytes with antibody markers, as above, before ethanol fixation and 10μg/mL DAPI staining prior to flow cytometry.

Apoptosis assay.—Cell death analyses were completed by harvesting organs and staining cell surface antigens before incubation with annexin V binding buffer (10 mM HEPES, 150 mM NaCl, 2.5 mM $CaCl_2$). Cells were then washed and incubated in 5μL per sample annexin V- FITC in annexin V binding buffer before a final wash and incubation in annexin V binding buffer with 0.01μg/mL DAPI before analysis on LSRII flow cytometer. Analysis was completed using FlowJo analysis software (BD Biosciences). Using light scatter and viability dyes, all cells were gated on live, singlet, lymphocytes before further analysis. The numbers of cells in each individual population were compared between genotypes and analyzed using GraphPad Prism.

Phosphospecific Flow Cytometry: For measurement of PI-3-K, ERK1/2, AKT, and SYK activation in transduced cell lines, Fc receptor-deficient A20IIA1.6 B cells were serum-starved by incubation for 2 hours in DMEM with 2% FCS, followed by 1 hour in serum-free media. 2×10^6 cells were stimulated with 400,000 Tosylactivated Dynabeads M-450 magnetic beads (ThermoFisher Scientific) conjugated to anti-κ light chain antibody (187.1, Bio X Cell) according to the manufacturer protocol. Cells were stimulated at 37°C for the times indicated in the figures, and then fixed in 1.4% paraformaldahyde (PFA) for 10 minutes at room temperature and permeabilized with cold 100% methanol for 20 minutes on ice. Cells were stained with PE conjugated anti-pPI3K p85/p55 (PI3KY458–1A11, Invitrogen), AlexaFluor-488 conjugated anti-pERK1/2 (4B11B69, Biolegend), PE conjugated pAkt Ser473 (D9E, Cell Signaling Technology) and APC conjugated anti-pSYK (moch1ct, eBioscience) for 30 minutes at room temperature. Samples were analyzed on an LSRII flow cytometer. Analysis was completed using FlowJo analysis software. For measurement of ERK activation in stimulated primary B cells, splenic B cells were isolated from mice using the MojoSort Mouse Pan B Cell Isolation Kit (Biolegend). After isolation,

B cells were serum starved by incubation for 2 hours in DMEM with 2% FCS, followed by 1 hour in serum-free media. For stimulation, 2×10^6 B cells were stimulated with 10 μg/mL goat F(ab')2 anti-mouse Ig (H+L) (Southern Biotech). Cells were gated on live singlets before further analysis. Mean fluorescence intensity (MFI) was calculated using FlowJo software and statistically analyzed using GraphPad Prism. For examination of phospho-ERK in splenocytes of naïve mice, spleens were harvested and disaggregated directly into 1.4% paraformaldehyde in PBS.

Quantification and Statistical Analysis

Statistical information regarding sample sizes, statistical tests used and p-values are specified in figure captions. A significance level cutoff of $p<0.05$ was used in all experiments. Sample sizes were determined based on power calculations from pilot studies. Densitometry was done using ImageJ software. Quantitative data were analyzed on GraphPad Prism as specified above or as described in figure legends.

Results

Tyrosine 281 of FCRL1 mediates phosphorylation-dependent recruitment of GRB2, GRAP, and SHIP-1.

To determine the mechanism by which FCRL1 signals for B cell activation, lentiviral expression vectors were used to express site-directed FCRL1 mutants in which cytoplasmic tyrosine residues were substituted with phenylalanine (Figure 1A). FLAG epitope-tagged constructs encoding wild-type or mutated FCRL1 were transduced into the FcγRIIb-deficient A20.IIA1.6 (A20) cell line. Immunoprecipitation of the FLAG epitope from pervanadate-treated cells was performed and associated proteins were identified by liquid chromatography coupled to tandem mass spectrometry (LC-MS-MS). Immunoprecipitation of FLAG from parental A20, A20 expressing wild-type FCRL1 (WT), and A20 expressing FCRL1 with all six cytoplasmic tyrosines changed to phenylalanine (6YF) cell lines revealed that FCRL1 associates with the adaptor proteins GRB2 and GRAP, as well as the phosphoinositide phosphatase SHIP-1 and the guanine nucleotide exchange factor SOS1, in a phosphotyrosine-dependent manner (Figure 1B). Phosphorylation of FCRL1 cytoplasmic tyrosines 281 and 297 was directly observed in the mass spectrometry experiments (Supplementary Figure 3), implicating these two residues as potential docking sites for SH2 domain-containing proteins.

Site-directed mutagenesis was used to introduce point mutations into FCRL1 for the determination of tyrosine residues necessary for binding partner recruitment. Point mutations were directed to Y_{281} and Y_{297}, along with the other 4 tyrosines found within the cytoplasmic tail of FCRL1. To avoid potentially confounding effects of native FCRL1 in A20 cells, *Fcrl1*−/− A20.IIA1.6 cells (A20.*ΔFcrl1*) were generated by Cas9-mediated targeting of *Fcrl1* (Figure S1A,B). To rescue FCRL1 expression without interference by Cas9, codon-optimized WT and site-directed mutants of FCRL1 were then expressed in the FCRL1 deficient A20 cells by lentiviral transduction. Immunoprecipitation and western blotting for phosphotyrosine in the WT, $Y_{281}F$, and $Y_{297}F$ exhibited tyrosine phosphorylation of a 72 kDa protein which was not observed in the 6YF

immunoprecipitated sample (Figure 1D). These data confirmed the mass spectrometry results that indicated phosphorylation of Y_{281} and Y_{297}. It is notable that the expected molecular weight of FCRL1 under reducing and denaturing SDS-PAGE is 36.5 kDa, yet blots for anti-FLAG or anti-pTyr consistently yield a band corresponding to FLAG-tagged FCRL1 at 72 kDa. No bands for pTyr or FLAG are found in FCRL1-expressing cells at 36 kDa. To verify that the 72 kDa band is FCRL1, a monoclonal antibody was generated against the C-terminus of mouse FCRL1 and used for western blotting of immunoprecipitated native FCRL1 in A20 cells and primary mouse splenocytes. A 72 kDa band was again observed in immunoprecipitate from wild-type, but not *Fcrl1−/−* cells (Supplementary Figure 1C). We therefore confirm that the 72 kDa band is FCRL1, despite its appearance at approximately twice the expected size. While slow migration during SDS-PAGE is common among membrane proteins, it is not yet clear whether the observed size of FCRL1 during SDS-PAGE is a result of post-translational modifications, formation of a SDS-stable dimer, anomalous interactions with SDS, or some combination of factors.

To confirm the association of signaling proteins identified by LC-MS-MS, the pervanadate-treated samples immunoprecipitated with anti-FLAG were immunoblotted for GRB2, SOS1, and SHIP-1. All three proteins were observed to co-precipitate with native FCRL1 (Figure 1C). To examine the contributions of individual tyrosine residues to phosphorylation of FCRL1 and recruitment of downstream signaling partners, site directed mutants with tyrosine 281, 297, or all 6 tyrosines changed to phenylalanine were transduced into A20*ΔFcrl1* cells. The co-precipitation of these binding partners was abolished in Y_{281}F and 6YF immunoprecipitated samples, suggesting that Y_{281} is necessary for the recruitment of GRB2, SOS1, and SHIP-1 (Figure 1D). Commercially available antibodies to the other identified binding partner, GRAP, were found to be non-specific or cross-reactive to GRB2. As a result, GRAP association with FCRL1 has not yet been confirmed by western blotting. GRAP-specific monoclonal antibodies are currently in development.

GRB2 and SHIP-1 both contain SH2 domains that may mediate their association with Y_{281} of FCRL1. Furthermore, SHIP-1 contains multiple PxxP motifs that could serve as docking sites for the SH3 domains of GRB-2. Therefore, the dependency of GRB2 and SHIP-1 binding on the same tyrosine residue provoked inquiry into whether their interactions were dependent or competitive. To differentiate between these possibilities, we used CRISPR-Cas9 to target *Grb2* in the A20.IIA1.6 cell line (Figure S1E), and GRB2 deficiency was confirmed by western blot. FLAG-tagged wild-type FCRL1 was subsequently transduced into the *Grb2−/− (ΔGrb2)* cell line. Immunoprecipitation of the FLAG epitope from *Grb2−/−* cell line coupled with immunoblotting for SHIP-1 and SOS-1 indicated that GRB2 deficiency abrogated the associations of SHIP-1 and SOS-1 with FCRL1 (Figure 1E). Therefore, SOS-1 and SHIP-1 binding to FCRL1 are indirect and dependent on GRB2. A previously described interaction between an SH3 domain of GRB2 and the proline-rich C-terminus of SHIP-1 could account for this indirect interaction between SHIP-1 and FCRL1 (48–51).

Pharmacological phosphatase inhibition with pervanadate allows all potential phosphotyrosine interactors to associate, but does not provide information on the biological context of the association. To examine which proteins associate with FCRL1 in the context

of BCR cross-linking, A20 cells were stimulated with goat $F(ab')_2$ anti-mouse Ig prior to immunoprecipitation. BCR stimulation induced tyrosine phosphorylation of FCRL1 and recruitment of GRB2, however, SHIP-1 recruitment was only very weakly observed, and SOS1 was not observed to be associated with FCRL1 under these conditions (Figure 1F), suggesting that efficient SHIP-1 and SOS1 recruitment may require additional co-stimulatory signals.

FCRL1 inhibits ERK phosphorylation in A20 cells.

Since GRB2/SOS1 recruitment by FCRL1 was observed, and GRB2 and GRAP are reported to potentiate ERK phosphorylation in human B cells (52), we hypothesized that recruitment of GRB2 to FCRL1 would augment ERK1/2 phosphorylation downstream of BCR stimulus. To test this hypothesis, phospho-ERK1/2 in A20 B cells was analyzed by intracellular flow cytometry after crosslinking the B cell receptor with anti-kappa light chain antibodies immobilized on beads. Surprisingly, FCRL1 negatively regulated ERK phosphorylation in a tyrosine-dependent manner, with peak ERK1/2 phosphorylation and FCRL1-mediated inhibition observable 10 minutes after BCR cross-linking. Compared with parental A20 cells, A20.*ΔFcrl1* had significantly increased ERK activation following BCR stimulation. By contrast, over-expression of wild-type FCRL1 in the *ΔFcrl1* A20 cells led to robust suppression of ERK phosphorylation downstream of BCR engagement that was mostly abrogated in the 6YF mutant (Figure 2A). Both Y_{281} and Y_{297} were required for maximal ERK inhibition as loss of either tyrosine was sufficient to abrogate ERK suppression (Figure 2B). This indicates that FCRL1 suppresses ERK activation, and that suppression is mediated through Y_{281} as well as unidentified binding partners recruited to Y_{297}.

A previous report has shown that FCRL1 co-localizes with the BCR after BCR cross-linking and has implicated FCRL1 in activation of SYK and PI-3-kinase after B cell receptor engagement (45). To examine whether FCRL1 inhibits ERK phosphorylation while simultaneously activating phosphorylation of other signaling mediators such as SYK, Akt, and PI-3-kinase, phosphorylation of these proteins was measured by intracellular flow cytometry at the same time as ERK phosphorylation. No significant impacts of FCRL1 were observed in A20 cells on total Akt, SYK or PI-3-kinase phosphorylation (Figure 2C).

To examine whether the inhibitory effect of FCRL1 was dependent on GRB2 recruitment, GRB2 deficient (*ΔGrb2*) A20 cells were generated and stimulated as above. In addition, a fusion construct of GRB2 and FCRL1.6YF was generated and transduced into A20.*ΔFcrl1* cells to generate expression of GRB2 fused to the C-terminus of tyrosine-mutated FCRL1 (Figure 2D). In a manner comparable to that observed in A20ΔFcrl1 cells, ERK phosphorylation levels were increased in BCR-stimulated ΔGrb2 cells relative to parental A20 cells. Furthermore, the covalent attachment of GRB2 to FCRL1 was found to be sufficient for suppression of ERK activation at a level comparable to over-expressed wild-type FCRL1 (Figure 2E). These data indicate that GRB2 recruitment is crucial for FCRL1-mediated ERK suppression.

FCRL1 expression begins in immature B cells and continues throughout development and activation.

Signaling through ERK1/2 and ERK5 are known to impact B cell growth and survival (21, 53), and FCRL1 has been reported to positively contribute to B-cell activation in humans and mice (44, 45). Therefore, it is possible that FCRL1 suppression of ERK activation is modulating B cell responses to antigen. However, because the cellular expression pattern of FCRL1 in mice has not been established, it is unclear in which populations of B cells this role may be important. To establish the relevance of these findings in primary B cells, flow cytometry was used to define which populations of B cells express FCRL1. To characterize FCRL1 expression in lymphoid tissues, bone marrow and spleens were harvested from WT and *Fcrl1−/−* age- and sex-matched 129/SvImJ mice. In bone marrow, no FCRL1 expression was observed on pro-B cells ($B220^{lo}VpreB^{-}CD24^{-}$), while pre-B cells ($B220^{lo}VpreB^{+}CD24^{+}$) had very low or negligible FCRL1 expression (Figure 3B). FCRL1 expression is upregulated upon transition to the immature B cell stage ($B220^{+}AA4.1^{+}$), and expression remains high as development progresses in the spleen through immature transitional 1 (T1) ($B220^{+}AA4.1^{+}IgM^{hi}CD23^{-}$), transitional 2 (T2) ($B220^{+}AA4.1^{+}IgM^{hi}CD23^{+}$), transitional 3 (T3) ($B220^{+}AA4.1^{+}IgM^{lo}CD23^{+}$), and mature ($B220^{+}AA4.1^{-}$) B cell stages (Figure 3A). However, expression decreases on germinal center B cells ($B220^{+}AA4.1^{+}IgD^{-}GL7^{+}$) and plasma cells ($CD138^{++}$) (Figure 3). In comparison with a published report of FCRL1 expression in human tonsillar B cells, (44) these results indicate that the expression pattern of mouse and human FCRL1 in B cells is largely conserved.

FCRL1 suppresses ERK activation in primary mouse B cells.

With the data in A20 cells implicating FCRL1 in controlling ERK activation downstream of the BCR, and observations in mice showing FCRL1 expression in peripheral B cells, we set out to measure whether FCRL1 would impact ERK activation in primary B cells. Primary splenic B cells from WT and *Fcrl1−/−* mice were purified by magnetic enrichment using negative selection and then stimulated ex vivo using polyclonal $F(ab')_2$ anti-mouse Ig antibodies to detect levels of ERK phosphorylation by intracellular flow cytometry. In response to BCR crosslinking, the highest ERK phosphorylation was found in immature B cells, however, FCRL1 inhibited ERK in both immature and mature B cells after BCR engagement (Figure 4A, B). No impact of FCRL1 on SYK, Akt, or PI-3-kinase phosphorylation was observed under these conditions.

To examine whether ERK inhibition by FCRL1 occurs in vivo, spleens were removed from naïve WT and *Fcrl1−/−* mice and disaggregated directly into fixative. ERK phosphorylation was again measured by intracellular flow cytometry. Although the overall magnitude of ERK phosphorylation was lower in freshly fixed B cells compared with those that had been stimulated ex vivo, *Fcrl1* $^{-/-}$ B cells still exhibited significantly higher ERK phosphorylation than WT controls. This was true for mature and immature B cells. Again, no significant differences were consistently observed in levels of SYK or PI-3-kinase phosphorylation in these assays (Figure 4C, D). Overall, these data indicate a role for FCRL1 in regulating ERK phosphorylation in primary B cells, even during tonic signaling.

FCRL1 impacts late B lymphopoiesis.

We have shown that FCRL1 is expressed on immature B cells in the spleen and modulates ERK activity in B cell lines and primary splenic B cells, including immature B cells. Since ERK is known to promote B cell maturation in the spleen (54), we hypothesized that FCRL1 may play a role in regulating B cell maturation. To assess this possibility, bone marrow and spleens were harvested from naive age- and sex-matched WT and *Fcrl1* −/− mice and analyzed for B cell developmental population frequencies. Multiparametric flow cytometry was used to determine the number and developmental stage of cells. Compared to WT mice, *Fcrl1* −/− mice exhibited significantly increased numbers of splenic mature and immature B cells. The difference in immature B cell numbers could largely be accounted for by those in the T3 stage, and increases in mature B cells in *Fcrl1*−/− mice were found in naive follicular ($B220^+AA4.1^-CD23^+$) and marginal zone ($B220^+AA4.1^-IgM^+CD23^{-/low}$) B cells (Figure 5A).

To examine whether the increased numbers of splenic B cells in *Fcrl1*−/− mice was the result of increased proliferation during maturation, naïve mice were injected with BrdU to label proliferating B cells. Splenic B cell subsets delineated as in Figure 3 were then assayed by intracellular flow cytometry for BrdU incorporation. Significant increases in BrdU+ immature B cells were seen in *Fcrl1*−/− mice across all transitional stages. Among mature B cells, increased numbers of BrdU+ follicular and germinal center B cells were observed in *Fcrl1*−/− mice compared with controls (Figure 5B). Since normal splenic immature B cells and mature naïve B cells have been shown to be non-proliferating (55–57), flow cytometric cell cycle analysis was performed to determine whether the increase in BrdU+ B cells in *Fcrl1*−/− mice was linked to dysregulated cell cycle control. Cell cycle progression in WT and *Fcrl1*−/− splenic B cells was consistent with prior data indicating negligible proliferation in immature and naïve mature populations, while bone marrow populations had significant proliferation (55), and no differences between genotypes was observed (Figure 5C). This indicates that increased numbers of BrdU+ B cells in *Fcrl1*−/− mice is not the result of increased proliferation. To examine whether differences in cell death could account for the increased cell numbers in *Fcrl1* −/− mice. Annexin V and propidium iodide staining of WT and *Fcrl1* −/− splenocytes showed that *Fcrl1*−/− mice had significantly fewer apoptotic immature and naïve follicular B cells than WT controls (Figure 5D), implicating FCRL1 in regulation of B cell survival in response to tonic signals. While the BrdU incorporation data leave open the possibility of a role for FCRL1 in controlling the rate of B cell progression through immature stages, the difference in percentages of apoptotic cells demonstrate a role for FCRL1 in regulating splenic B cell numbers, in part, through modulation of apoptotic signals.

Discussion

FCRL1 is an activating co-receptor in the BCR signaling pathway. While its roles in augmenting calcium flux, B cell proliferation, and B cell synapse formation in response to antigen receptor stimulation have been reported previously (44, 45), our investigation of the role of FCRL1 in B cell signaling and activation revealed an unexpected inhibitory function in MAPK regulation downstream of BCR cross-linking. Mouse FCRL1 displays one ITAM

(ExxYxxVx_6ExYxxV) in its cytoplasmic domain (58) along with a second sequence with ITAM-like spacing between the tyrosines (YxxPx_8YxxA). With the presence of potential ITAMs and the previously reported activating functions of the receptor, we expected to see recruitment of SYK upon phosphorylation of the receptor. No such recruitment was observed, so immunoprecipitation coupled with mass-spectrometry analysis was undertaken to identify functional phosphorylation sites and novel associations. Of the tyrosines found within the canonical ITAM sequence, it is notable that we directly observed phosphorylation of only the first tyrosine, Y_{281}. This observation, coupled with the suppressive signaling that we observed, may indicate that the cytoplasmic tail of FCRL1 exhibits a role analogous to inhibitory ITAM (ITAMi) function (59).

Mechanistically, FCRL1-mediated ERK inhibition through a GRB2/SHIP-1 signaling module will require further analysis to completely define. Although our description of the inhibitory capacity of FCRL1 is novel, it is broadly consistent with previous observations on the roles of GRB2, GRAP, and SHIP-1 in B cell signaling. In the context of B cell signaling networks, GRB2 is highly pleotropic, with signal modulatory functions that extend to antigen-receptor signaling, as well as cytokine signaling networks, and do not fit neatly into an activating or inhibitory paradigm. (10, 52, 60, 61). SHIP-1 and GRB2 are each required to be recruited to the BCR complex for proper formation of central supramolecular activation clusters (62, 63), and FCRL1 is recruited to the B cell synapse upon BCR cross-linking and is required for maximum BCR clustering (45). Thus, GRB2 recruitment to FCRL1, potentially together with SHIP-1, may contribute to the formation of supramolecular activation clusters found during B cell activation.

Our results finding ERK inhibition by FCRL1 were found under conditions identical to those that are reported to produce enhanced calcium flux by this receptor (Supplementary Figure 2) (44, 45). Therefore, it is necessary to consider whether the same signaling pathway could be producing both effects simultaneously. A GRB2/SHIP-1 signaling module has the capacity to negatively regulate ERK activation through a variety of mechanisms. The inositol phosphatase activity of SHIP-1 may function to reduce the ratio of PI(3,4,5)P_3 to PI(3,4)P_2, diminishing PLC recruitment to the immune synapse to downregulate the downstream MAP kinase pathway (49–51). Alternatively, phosphatase-independent functions of SHIP-1 entail recruitment of RasGAPs to BCR complexes and destabilization of GRB2/Shc/SOS complexes, attenuating ERK activation (64, 65). Although the role of GRB2 in regulating ERK signaling in B cells has been a subject of some controversy (60, 62), several mechanisms whereby GRB2 could independently mediate ERK inhibition have been proposed. These include both spatiotemporal regulation of ERK activation and allosteric changes in SOS-1 upon GRB2 binding that reduce its GEF activity (66, 67). While SOS-1 activity is reported to be dispensable in mouse lymphocytes, it has been suggested that SOS-mediated positive feedback is required for responses to physiological antigen concentrations (68). While GRB2, SHIP-1, and SOS can all be recruited to Y_{281}, our finding that Y_{297} is also required for ERK inhibition suggests a currently uncharacterized inhibitory pathway involving an unidentified binding partner that is recruited to Y_{297}. In T cells, GRAP has been demonstrated to negatively regulate ERK downstream of Ras activation through an unknown mechanism, making it tempting to speculate that GRAP contributes to such a pathway coordinated by FCRL1 (69).

An earlier study using over-expression of both FCRL1 and c-ABL in B cells implicated recruitment of c-ABL to FCRL1 Y_{281} to mediate its activating role (45). We were unable to replicate these findings by immunoprecipitation in A20 B cells that express native c-ABL, even when the expression of a potential binding-site competitor, GRB2, was ablated. We conclude that any FCRL1/c-ABL interaction may be low affinity or very transient under endogenous concentrations of c-ABL in the cell. Future quantitative biochemical analyses will be required to address this discrepancy. The same study also showed a role for FCRL1 in generating adaptive immune responses, with *Fcrl1*$^{-/-}$ mice showing impaired development of antigen-specific antibodies after immunization with thymus-dependent and thymus-independent antigens. We observed the same phenomena in our mice (not shown), indicating that differences between our results are unlikely to be the result of strain differences between the mice. In another potential contrast to the findings of Zhao et al. that reported FCRL1-dependent enhancement of synaptic SYK and PI-3-kinase phosphorylation (45), we did not observe FCRL1-dependent changes to total SYK and PI-3-kinase phosphorylation upon BCR engagement. However, the differences in outcomes may be linked to methodology. While both studies used an immobilized cross-linker of the BCR and identical stimulation times, this study used intracellular flow cytometry to measure *total* SYK and PI-3-kinase phosphorylation, whereas Zhao et al. used imaging to examine phosphoproteins within the B cell synapse. Furthermore, in quantifying the level of signal, Zhao et al. defined mean fluorescence intensity (mFI) not by the total fluorescence intensity (TFI), but rather as the TFI divided by the area of the contact interface (45). As such, relative decreases in the size of the contact interface would have a similar mathematical effect on calculated ‘mFI’ as increases in the TFI signal. Thus, the interpreted FCRL1-dependent increase in phosphorylation of SYK, PI3-K, and BLNK may have reflected FCRL1-mediated reductions to the BCR contact interface rather than increases in phosphorylation. Further studies would be required to examine this possibility and to dissect the impacts of FCRL1-mediated recruitment of c-Abl, GRB2, GRAP, SOS-1, and SHIP-1 during B cell maturation and differentiation.

Although our data show that FCRL1 expression remains undetectable or low in pro-B cells and pre-B cells in the bone marrow, its expression in splenic immature and transitional B cell populations suggests a role in peripheral maintenance of B cells, and we observed both reduced apoptosis and enhanced ERK activity in the absence of FCRL1 in transitional and mature splenic B cells at a resting state. Ras activation upstream of ERK has been found to promote maturation of immature B cells, with late transitional, mature, and activated B cells undergoing proliferation and differentiation upon ERK pathway activation (54). The elevated B cell counts, increased BrdU incorporation of maturing B cells, reduced apoptosis, and elevated resting state phospho-ERK levels in *Fcrl1*$^{-/-}$ mice invite the possibility that FCRL1 is involved in maintaining peripheral tolerance, as dysregulated Ras activation has been linked to failure to select against autoreactive immature B cells (70). Likewise, the increased counts of plasma cells in *Fcrl1*$^{-/-}$ mice are consistent with the requirement of ERK for PAX5 phosphorylation and *Blimp1* upregulation during plasma cell differentiation (71). Further studies will be required to determine whether the regulation of B cell numbers by FCRL1 during splenic B cell maturation plays a role in negative selection of autoreactive B cells.

In summary, our characterization of FCRL1 as a negative regulator of ERK activity suggests that FCRL1 serves a complex immunomodulatory role in B cell signaling, transducing both activating and inhibitory signals downstream of antigen receptor engagement. We propose that the GRB2/SHIP-1 signaling complex recruited to the Y_{281}ENV motif is partially responsible for the inhibitory capacity of FCRL1, although our observation that Y_{297} is necessary for ERK inhibition invites the possibility that currently unidentified interactors involved in this pathway remain to be discovered. Our data suggest that the contributions of FCRL1 to B cell signaling may regulate peripheral selection in immature and transitional B cells, where over-activation of ERK may be contributing to dysregulated cellularity. However, the physiological impact of FCRL1 shifts dramatically in the context of the antigenic challenge, in which *Fcrl1*$^{-/-}$ mice demonstrate impaired specific antibody production. This seemingly paradoxical role of FCRL1 warrants continued exploration into its role in B cell activation and differentiation.

Supplementary Material

Refer to Web version on PubMed Central for supplementary material.

Acknowledgements

We would like to thank John Cambier for the generous gift of A20IIA1.6 cells. Instrumentation support was provided by the Center for Bioinformatics and Functional Genomics at Miami University along with the NMR/MS Instrumentation Facility at Miami University, specifically Theresa Ramelot.

Funding was provided by NSF-MRI #1726643, Miami University intramural start-up funds, and the Committee on Faculty Research. J.M.D. and T.J.W. received salary support from NIH R15-AI138184. M.K.M was supported by a University Summer Scholarship, HHMI Summer Scholarship, and Dean's Scholarship, and M.K.M and J.M.D. were supported by a Miami University DUOS award.

REFERENCES

1. Fulcher DA, and Basten A. 1994. Whither the anergic B-cell? Autoimmunity 19: 135–140. [PubMed: 7772703]
2. Qian Y, Santiago C, Borrero M, Tedder TF, and Clarke SH. 2001. Lupus-specific antiribonucleoprotein B cell tolerance in nonautoimmune mice is maintained by differentiation to B-1 and governed by B cell receptor signaling thresholds. J Immunol 166: 2412–2419. [PubMed: 11160300]
3. Soto L, Ferrier A, Aravena O, Fonseca E, Berendsen J, Biere A, Bueno D, Ramos V, Aguillon JC, and Catalan D. 2015. Systemic Sclerosis Patients Present Alterations in the Expression of Molecules Involved in B-Cell Regulation. Front Immunol 6: 496. [PubMed: 26483788]
4. Luo W, Weisel F, and Shlomchik MJ. 2018. B Cell Receptor and CD40 Signaling Are Rewired for Synergistic Induction of the c-Myc Transcription Factor in Germinal Center B Cells. Immunity 48: 313–326 e315. [PubMed: 29396161]
5. Luo W, Mayeux J, Gutierrez T, Russell L, Getahun A, Muller J, Tedder T, Parnes J, Rickert R, Nitschke L, Cambier J, Satterthwaite AB, and Garrett-Sinha LA. 2014. A balance between B cell receptor and inhibitory receptor signaling controls plasma cell differentiation by maintaining optimal Ets1 levels. J Immunol 193: 909–920. [PubMed: 24929000]
6. Heltemes LM, and Manser T. 2002. Level of B cell antigen receptor surface expression influences both positive and negative selection of B cells during primary development. J Immunol 169: 1283–1292. [PubMed: 12133950]

7. Gross AJ, Lyandres JR, Panigrahi AK, Prak ET, and DeFranco AL. 2009. Developmental acquisition of the Lyn-CD22-SHP-1 inhibitory pathway promotes B cell tolerance. J Immunol 182: 5382–5392. [PubMed: 19380785]

8. Wheeler ML, Dong MB, Brink R, Zhong XP, and DeFranco AL. 2013. Diacylglycerol kinase zeta limits B cell antigen receptor-dependent activation of ERK signaling to inhibit early antibody responses. Sci Signal 6: ra91. [PubMed: 24129701]

9. Limnander A, and Weiss A. 2011. Ca-dependent Ras/Erk signaling mediates negative selection of autoreactive B cells. Small GTPases 2: 282–288. [PubMed: 22292132]

10. Stork B, Engelke M, Frey J, Horejsi V, Hamm-Baarke A, Schraven B, Kurosaki T, and Wienands J. 2004. Grb2 and the non-T cell activation linker NTAL constitute a Ca(2+)-regulating signal circuit in B lymphocytes. Immunity 21: 681–691. [PubMed: 15539154]

11. Rowland SL, Leahy KF, Halverson R, Torres RM, and Pelanda R. 2010. BAFF receptor signaling aids the differentiation of immature B cells into transitional B cells following tonic BCR signaling. J Immunol 185: 4570–4581. [PubMed: 20861359]

12. Schiemann B, Gommerman JL, Vora K, Cachero TG, Shulga-Morskaya S, Dobles M, Frew E, and Scott ML. 2001. An essential role for BAFF in the normal development of B cells through a BCMA-independent pathway. Science 293: 2111–2114. [PubMed: 11509691]

13. Yan M, Brady JR, Chan B, Lee WP, Hsu B, Harless S, Cancro M, Grewal IS, and Dixit VM. 2001. Identification of a novel receptor for B lymphocyte stimulator that is mutated in a mouse strain with severe B cell deficiency. Curr Biol 11: 1547–1552. [PubMed: 11591325]

14. Rawlings DJ, Metzler G, Wray-Dutra M, and Jackson SW. 2017. Altered B cell signalling in autoimmunity. Nat Rev Immunol 17: 421–436. [PubMed: 28393923]

15. Lin J, and Justement LB. 1992. The MB-1/B29 heterodimer couples the B cell antigen receptor to multiple src family protein tyrosine kinases. J Immunol 149: 1548–1555. [PubMed: 1506682]

16. Jugloff LS, and Jongstra-Bilen J. 1997. Cross-linking of the IgM receptor induces rapid translocation of IgM-associated Ig alpha, Lyn, and Syk tyrosine kinases to the membrane skeleton. J Immunol 159: 1096–1106. [PubMed: 9233602]

17. Beitz LO, Fruman DA, Kurosaki T, Cantley LC, and Scharenberg AM. 1999. SYK is upstream of phosphoinositide 3-kinase in B cell receptor signaling. J Biol Chem 274: 32662–32666. [PubMed: 10551821]

18. Okada T, Maeda A, Iwamatsu A, Gotoh K, and Kurosaki T. 2000. BCAP: the tyrosine kinase substrate that connects B cell receptor to phosphoinositide 3-kinase activation. Immunity 13: 817–827. [PubMed: 11163197]

19. Fu C, Turck CW, Kurosaki T, and Chan AC. 1998. BLNK: a central linker protein in B cell activation. Immunity 9: 93–103. [PubMed: 9697839]

20. Packard TA, and Cambier JC. 2013. B lymphocyte antigen receptor signaling: initiation, amplification, and regulation. F1000Prime Rep 5: 40. [PubMed: 24167721]

21. Schweighoffer E, and Tybulewicz VL. 2018. Signalling for B cell survival. Curr Opin Cell Biol 51: 8–14. [PubMed: 29149682]

22. Wang LD, and Clark MR. 2003. B-cell antigen-receptor signalling in lymphocyte development. Immunology 110: 411–420. [PubMed: 14632637]

23. Ono M, Okada H, Bolland S, Yanagi S, Kurosaki T, and Ravetch JV. 1997. Deletion of SHIP or SHP-1 reveals two distinct pathways for inhibitory signaling. Cell 90: 293–301. [PubMed: 9244303]

24. Muraille E, Bruhns P, Pesesse X, Daeron M, and Erneux C. 2000. The SH2 domain containing inositol 5-phosphatase SHIP2 associates to the immunoreceptor tyrosine-based inhibition motif of Fc gammaRIIB in B cells under negative signaling. Immunol Lett 72: 7–15. [PubMed: 10789675]

25. Nakamura K, Malykhin A, and Coggeshall KM. 2002. The Src homology 2 domain-containing inositol 5-phosphatase negatively regulates Fcgamma receptor-mediated phagocytosis through immunoreceptor tyrosine-based activation motif-bearing phagocytic receptors. Blood 100: 3374–3382. [PubMed: 12384440]

26. Ganesan LP, Fang H, Marsh CB, and Tridandapani S. 2003. The protein-tyrosine phosphatase SHP-1 associates with the phosphorylated immunoreceptor tyrosine-based activation motif of Fc

gamma RIIa to modulate signaling events in myeloid cells. J Biol Chem 278: 35710–35717. [PubMed: 12832410]

27. Ehrhardt GR, and Cooper MD. 2011. Immunoregulatory roles for fc receptor-like molecules. Curr Top Microbiol Immunol 350: 89–104. [PubMed: 20680805]
28. Ehrhardt GR, Leu CM, Zhang S, Aksu G, Jackson T, Haga C, Hsu JT, Schreeder DM, Davis RS, and Cooper MD. 2007. Fc receptor-like proteins (FCRL): immunomodulators of B cell function. Adv Exp Med Biol 596: 155–162. [PubMed: 17338184]
29. Getahun A, and Cambier JC. 2015. Of ITIMs, ITAMs, and ITAMis: revisiting immunoglobulin Fc receptor signaling. Immunol Rev 268: 66–73. [PubMed: 26497513]
30. Jackson TA, Haga CL, Ehrhardt GR, Davis RS, and Cooper MD. 2010. FcR-like 2 Inhibition of B cell receptor-mediated activation of B cells. J Immunol 185: 7405–7412. [PubMed: 21068405]
31. Kulemzin SV, Zamoshnikova AY, Yurchenko MY, Vitak NY, Najakshin AM, Fayngerts SA, Chikaev NA, Reshetnikova ES, Kashirina NM, Peclo MM, Rutkevich PN, Shevelev AY, Yanushevskaya EV, Baranov KO, Mamonkin M, Vlasik TN, Sidorenko SP, Taranin AV, and Mechetina LV. 2011. FCRL6 receptor: expression and associated proteins. Immunol Lett 134: 174–182. [PubMed: 20933011]
32. Shabani M, Bayat AA, Jeddi-Tehrani M, Rabbani H, Hojjat-Farsangi M, Ulivieri C, Amirghofran Z, Baldari CT, and Shokri F. 2014. Ligation of human Fc receptor like-2 by monoclonal antibodies down-regulates B-cell receptor-mediated signalling. Immunology 143: 341–353. [PubMed: 24797767]
33. Wilson TJ, Presti RM, Tassi I, Overton ET, Cella M, and Colonna M. 2007. FcRL6, a new ITIM-bearing receptor on cytolytic cells, is broadly expressed by lymphocytes following HIV-1 infection. Blood 109: 3786–3793. [PubMed: 17213291]
34. Li FJ, Won WJ, Becker EJ Jr., Easlick JL, Tabengwa EM, Li R, Shakhmatov M, Honjo K, Burrows PD, and Davis RS. 2014. Emerging roles for the FCRL family members in lymphocyte biology and disease. Curr Top Microbiol Immunol 382: 29–50. [PubMed: 25116094]
35. Ehrhardt GR, Davis RS, Hsu JT, Leu CM, Ehrhardt A, and Cooper MD. 2003. The inhibitory potential of Fc receptor homolog 4 on memory B cells. Proc Natl Acad Sci U S A 100: 13489–13494. [PubMed: 14597715]
36. Franco A, Kraus Z, Li H, Seibert N, Dement-Brown J, and Tolnay M. 2018. CD21 and FCRL5 form a receptor complex with robust B-cell activating capacity. Int Immunol 30: 569–578. [PubMed: 30107486]
37. Haga CL, Ehrhardt GR, Boohaker RJ, Davis RS, and Cooper MD. 2007. Fc receptor-like 5 inhibits B cell activation via SHP-1 tyrosine phosphatase recruitment. Proc Natl Acad Sci U S A 104: 9770–9775. [PubMed: 17522256]
38. Liu Y, Bezverbnaya K, Zhao T, Parsons MJ, Shi M, Treanor B, and Ehrhardt GR. 2015. Involvement of the HCK and FGR src-family kinases in FCRL4-mediated immune regulation. J Immunol 194: 5851–5860. [PubMed: 25972488]
39. Sohn HW, Krueger PD, Davis RS, and Pierce SK. 2011. FcRL4 acts as an adaptive to innate molecular switch dampening BCR signaling and enhancing TLR signaling. Blood 118: 6332–6341. [PubMed: 21908428]
40. Zhu Z, Li R, Li H, Zhou T, and Davis RS. 2013. FCRL5 exerts binary and compartment-specific influence on innate-like B-cell receptor signaling. Proc Natl Acad Sci U S A 110: E1282–1290. [PubMed: 23509253]
41. Wilson TJ, Fuchs A, and Colonna M. 2012. Cutting edge: human FcRL4 and FcRL5 are receptors for IgA and IgG. J Immunol 188: 4741–4745. [PubMed: 22491254]
42. Agarwal S, Kraus Z, Dement-Brown J, Alabi O, Starost K, and Tolnay M. 2020. Human Fc Receptor-like 3 Inhibits Regulatory T Cell Function and Binds Secretory IgA. Cell Rep 30: 1292–1299 e1293. [PubMed: 32023449]
43. Liu Y, Goroshko S, Leung LYT, Dong S, Khan S, Campisi P, Propst EJ, Wolter NE, Grunebaum E, and Ehrhardt GRA. 2020. FCRL4 Is an Fc Receptor for Systemic IgA, but Not Mucosal Secretory IgA. J Immunol 205: 533–538. [PubMed: 32513851]
44. Leu CM, Davis RS, Gartland LA, Fine WD, and Cooper MD. 2005. FcRH1: an activation coreceptor on human B cells. Blood 105: 1121–1126. [PubMed: 15479727]

45. Zhao X, Xie H, Zhao M, Ahsan A, Li X, Wang F, Yi J, Yang Z, Wu C, Raman I, Li QZ, Kim TJ, and Liu W. 2019. Fc receptor-like 1 intrinsically recruits c-Abl to enhance B cell activation and function. Sci Adv 5: eaaw0315. [PubMed: 31328160]
46. Yousefi Z, Sharifzadeh S, Yar-Ahmadi V, Andalib A, and Eskandari N. 2019. Fc Receptor-Like 1 as a Promising Target for Immunotherapeutic Interventions of B-Cell-Related Disorders. Biomark Insights 14: 1177271919882351.
47. Carvalho PC, Lima DB, Leprevost FV, Santos MD, Fischer JS, Aquino PF, Moresco JJ, Yates JR 3rd, and Barbosa VC. 2016. Integrated analysis of shotgun proteomic data with PatternLab for proteomics 4.0. Nat Protoc 11: 102–117. [PubMed: 26658470]
48. Isnardi I, Lesourne R, Bruhns P, Fridman WH, Cambier JC, and Daeron M. 2004. Two distinct tyrosine-based motifs enable the inhibitory receptor FcgammaRIIB to cooperatively recruit the inositol phosphatases SHIP1/2 and the adapters Grb2/Grap. J Biol Chem 279: 51931–51938. [PubMed: 15456754]
49. Dowler S, Currie RA, Campbell DG, Deak M, Kular G, Downes CP, and Alessi DR. 2000. Identification of pleckstrin-homology-domain-containing proteins with novel phosphoinositide-binding specificities. Biochem J 351: 19–31. [PubMed: 11001876]
50. Bolland S, Pearse RN, Kurosaki T, and Ravetch JV. 1998. SHIP modulates immune receptor responses by regulating membrane association of Btk. Immunity 8: 509–516. [PubMed: 9586640]
51. Aman MJ, Lamkin TD, Okada H, Kurosaki T, and Ravichandran KS. 1998. The inositol phosphatase SHIP inhibits Akt/PKB activation in B cells. J Biol Chem 273: 33922–33928. [PubMed: 9852043]
52. Vanshylla K, Bartsch C, Hitzing C, Krumpelmann L, Wienands J, and Engels N. 2018. Grb2 and GRAP connect the B cell antigen receptor to Erk MAP kinase activation in human B cells. Sci Rep 8: 4244. [PubMed: 29523808]
53. Jacque E, Schweighoffer E, Tybulewicz VL, and Ley SC. 2015. BAFF activation of the ERK5 MAP kinase pathway regulates B cell survival. J Exp Med 212: 883–892. [PubMed: 25987726]
54. Rowland SL, DePersis CL, Torres RM, and Pelanda R. 2010. Ras activation of Erk restores impaired tonic BCR signaling and rescues immature B cell differentiation. J Exp Med 207: 607–621. [PubMed: 20176802]
55. Srivastava B, Quinn WJ 3rd, Hazard K, Erikson J, and Allman D. 2005. Characterization of marginal zone B cell precursors. J Exp Med 202: 1225–1234. [PubMed: 16260487]
56. Allman D, Lindsley RC, DeMuth W, Rudd K, Shinton SA, and Hardy RR. 2001. Resolution of three nonproliferative immature splenic B cell subsets reveals multiple selection points during peripheral B cell maturation. J Immunol 167: 6834–6840. [PubMed: 11739500]
57. Hsu BL, Harless SM, Lindsley RC, Hilbert DM, and Cancro MP. 2002. Cutting edge: BLyS enables survival of transitional and mature B cells through distinct mediators. J Immunol 168: 5993–5996. [PubMed: 12055205]
58. Reth M 1989. Antigen receptor tail clue. Nature 338: 383–384. [PubMed: 2927501]
59. Blank U, Launay P, Benhamou M, and Monteiro RC. 2009. Inhibitory ITAMs as novel regulators of immunity. Immunol Rev 232: 59–71. [PubMed: 19909356]
60. Ackermann JA, Radtke D, Maurberger A, Winkler TH, and Nitschke L. 2011. Grb2 regulates B-cell maturation, B-cell memory responses and inhibits B-cell Ca2+ signalling. EMBO J 30: 1621–1633. [PubMed: 21427701]
61. Jang IK, Cronshaw DG, Xie LK, Fang G, Zhang J, Oh H, Fu YX, Gu H, and Zou Y. 2011. Growth-factor receptor-bound protein-2 (Grb2) signaling in B cells controls lymphoid follicle organization and germinal center reaction. Proc Natl Acad Sci U S A 108: 7926–7931. [PubMed: 21508326]
62. Jiang X, Lu X, Zhang Y, Lacaria L, Schuchardt BJ, Mikles DC, Magistri M, Garcia-Ramirez I, Sanchez-Garcia I, Farooq A, Verdun RE, Abdulreda MH, Moy VT, and Lossos IS. 2019. Interplay between HGAL and Grb2 proteins regulates B-cell receptor signaling. Blood Adv 3: 2286–2297. [PubMed: 31362927]
63. Liu C, Miller H, Hui KL, Grooman B, Bolland S, Upadhyaya A, and Song W. 2011. A balance of Bruton's tyrosine kinase and SHIP activation regulates B cell receptor cluster formation by controlling actin remodeling. J Immunol 187: 230–239. [PubMed: 21622861]

64. Tamir I, Stolpa JC, Helgason CD, Nakamura K, Bruhns P, Daeron M, and Cambier JC. 2000. The RasGAP-binding protein p62dok is a mediator of inhibitory FcgammaRIIB signals in B cells. Immunity 12: 347–358. [PubMed: 10755621]

65. Tridandapani S, Kelley T, Cooney D, Pradhan M, and Coggeshall KM. 1997. Negative signaling in B cells: SHIP Grbs Shc. Immunol Today 18: 424–427. [PubMed: 9293157]

66. Yasuda T, and Kurosaki T. 2008. Regulation of lymphocyte fate by Ras/ERK signals. Cell Cycle 7: 3634–3640. [PubMed: 19029810]

67. Zarich N, Oliva JL, Martinez N, Jorge R, Ballester A, Gutierrez-Eisman S, Garcia-Vargas S, and Rojas JM. 2006. Grb2 is a negative modulator of the intrinsic Ras-GEF activity of hSos1. Mol Biol Cell 17: 3591–3597. [PubMed: 16760435]

68. Roose JP, Mollenauer M, Ho M, Kurosaki T, and Weiss A. 2007. Unusual interplay of two types of Ras activators, RasGRP and SOS, establishes sensitive and robust Ras activation in lymphocytes. Mol Cell Biol 27: 2732–2745. [PubMed: 17283063]

69. Shen R, Ouyang YB, Qu CK, Alonso A, Sperzel L, Mustelin T, Kaplan MH, and Feng GS. 2002. Grap negatively regulates T-cell receptor-elicited lymphocyte proliferation and interleukin-2 induction. Mol Cell Biol 22: 3230–3236. [PubMed: 11971956]

70. Teodorovic LS, Babolin C, Rowland SL, Greaves SA, Baldwin DP, Torres RM, and Pelanda R. 2014. Activation of Ras overcomes B-cell tolerance to promote differentiation of autoreactive B cells and production of autoantibodies. Proc Natl Acad Sci U S A 111: E2797–2806. [PubMed: 24958853]

71. Yasuda T, Hayakawa F, Kurahashi S, Sugimoto K, Minami Y, Tomita A, and Naoe T. 2012. B cell receptor-ERK1/2 signal cancels PAX5-dependent repression of BLIMP1 through PAX5 phosphorylation: a mechanism of antigen-triggering plasma cell differentiation. J Immunol 188: 6127–6134. [PubMed: 22593617]

Key Points

- FCRL1 recruits GRB2 to Y_{281} following BCR stimulus
- FCRL1 suppresses BCR-induced ERK1/2 phosphorylation through GRB2.
- FCRL1 controls transitional and mature B cell numbers and tonic ERK signals.

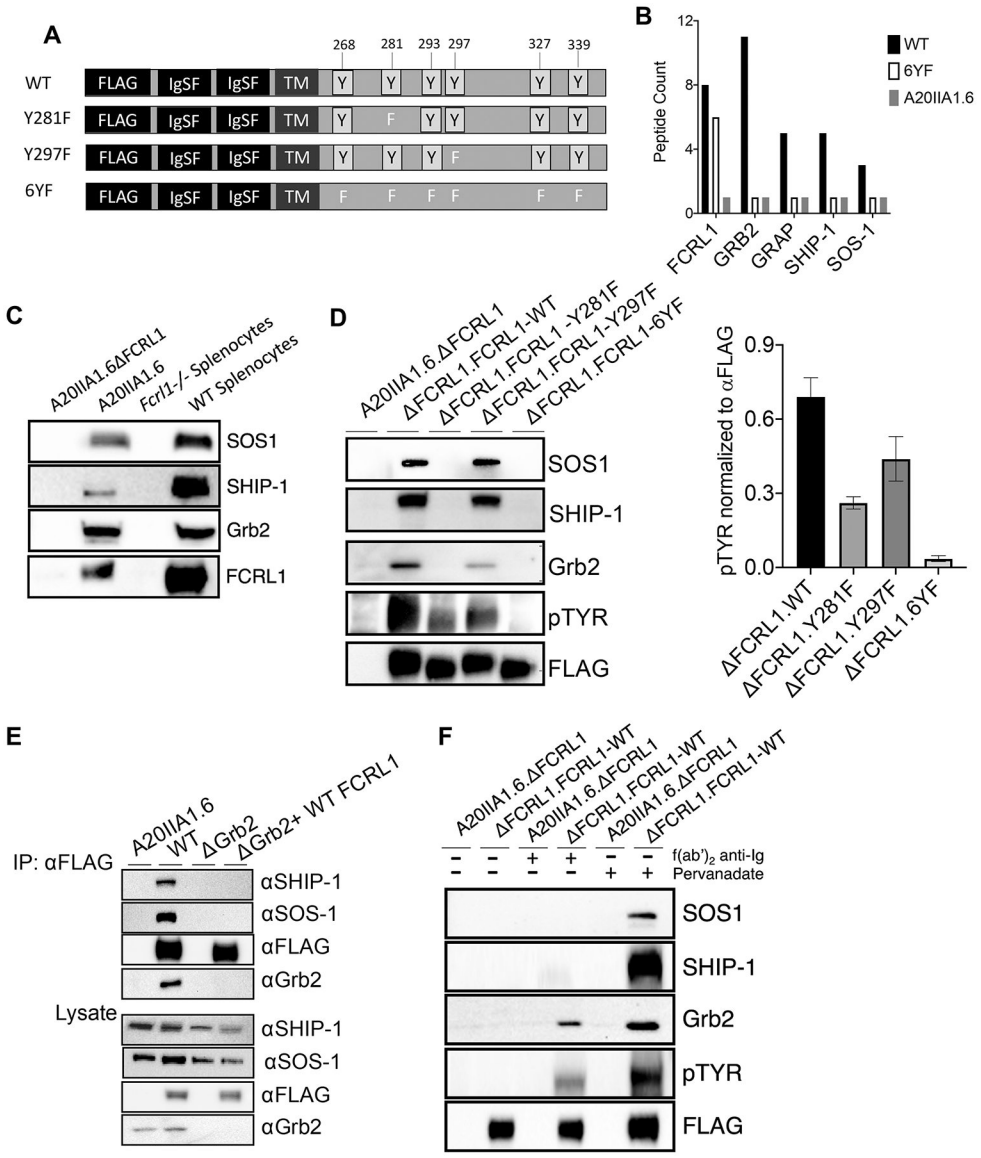

Figure 1. FCRL1 binds to Grb2, SHIP-1, and SOS-1.

(A) Schematics of FLAG-tagged WT FCRL1 and mutant proteins expressed in A20IIA1.6 parental and A20.*ΔFcrl1* B cells. IgSF = Immunoglobulin superfamily domain; TM = transmembrane region; Y indicates cytosolic tyrosine residue; numerical indicators for tyrosines are relative to the native initiator methionine of isoform 2. *(B)* Unique peptide counts recovered from mass spectrometric analysis of anti-FLAG immunoprecipitated lysates of pervanadate-activated WT, 6YF, and A20IIA1.6 parent line. These data are representative of two independent experiments. *(C)* Immunoblots of anti-FCRL1 precipitated lysates of pervanadate-treated A20 and A20.*ΔFcrl1* cell lines along with 129/SvImJ and *Fcrl1−/−* splenocytes. Results are representative of three independent experiments. *(D) Left,* Immunoblots of anti-FLAG precipitated lysates of pervanadate-treated A20.*ΔFcrl1* cell lines with rescued expression of WT or tyrosine-mutated FCRL1. Results are representative of three independent experiments. *Right*, relative densitometric

analysis of phospho-tyrosine normalized to anti-FLAG. *(E)* Immunoblots of anti-FLAG immunoprecipitated lysates of pervanadate-treated GRB2 deficient or sufficient A20IIa1.6 cells with or without expression of FLAG-tagged WT FCRL1. Data are representative of three independent experiments. *(F)* Immunoblots of anti-FLAG precipitated lysates of unstimulated, goat F(ab')2 anti-mouse Ig stimulated, or pervanadate-treated A20*ΔFcrl1* cell lines with rescued expression of WT FCRL1. Results are representative of three independent experiments.

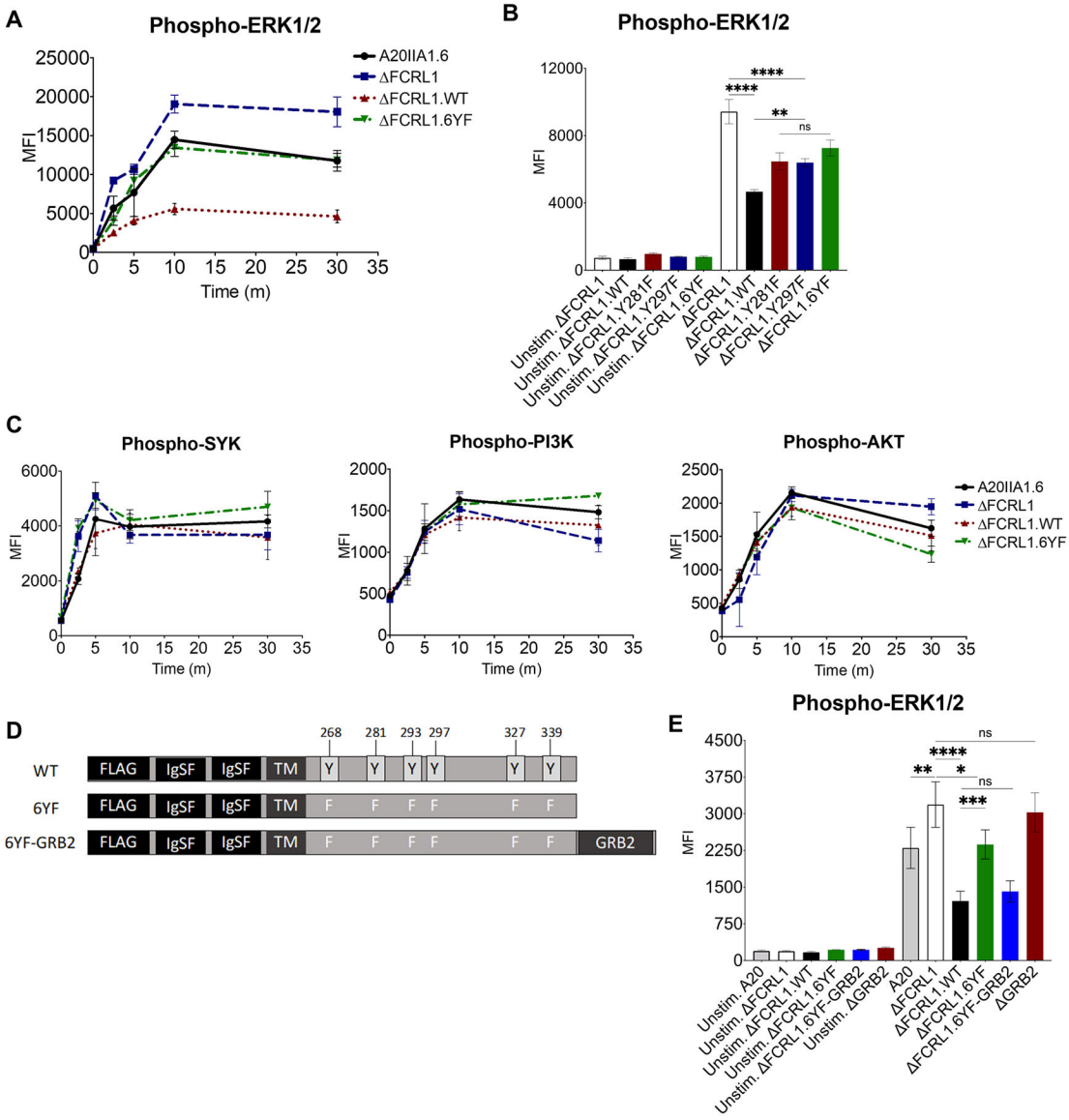

Figure 2. FCRL1 suppresses BCR-induced ERK activation.

(A) Flow cytometric quantitation of ERK1/2 phosphorylation after BCR crosslinking with anti-kappa light chain antibody-conjugated beads over time in A20IIA1.6 cells (black line), A20.*ΔFcrl1* cells (blue line), and cells with rescued expression of FCRL1 WT (red line) and 6YF (green line). *(B)* Flow cytometric quantitation of ERK1/2 phosphorylation before and after BCR crosslinking with anti-kappa light chain antibody-conjugated beads for 10 minutes in A20.*ΔFcrl1* cells with rescued expression of FCRL1 site-directed mutants. *(C)* Phosphorylation of SYK, PI-3-kinase, and AKT measured as in *(B)*. *(D)* Schematics of FLAG-tagged WT FCRL1, tyrosine-mutated (6YF), and fusion protein of tyrosine-mutated FCRL1 with GRB2, all expressed in A20.*ΔFcrl1* B cells. *(E)* Flow cytometric quantitation of ERK1/2 phosphorylation in parental and A20.*ΔFcrl1* cells, along with rescued FCRL1 WT, 6YF, and 6YF-GRB2 fusion expressing cells at 10 minutes post-stimulation. *(B,E)* Bars indicate the mean +/− SEM of biological triplicates. Data are representative of at least three

independent experiments. Statistical tests of means were performed using one-way ANOVA with Tukey's test for post-hoc analysis. *p<0.05, **p<0.005, ***p<0.0005.

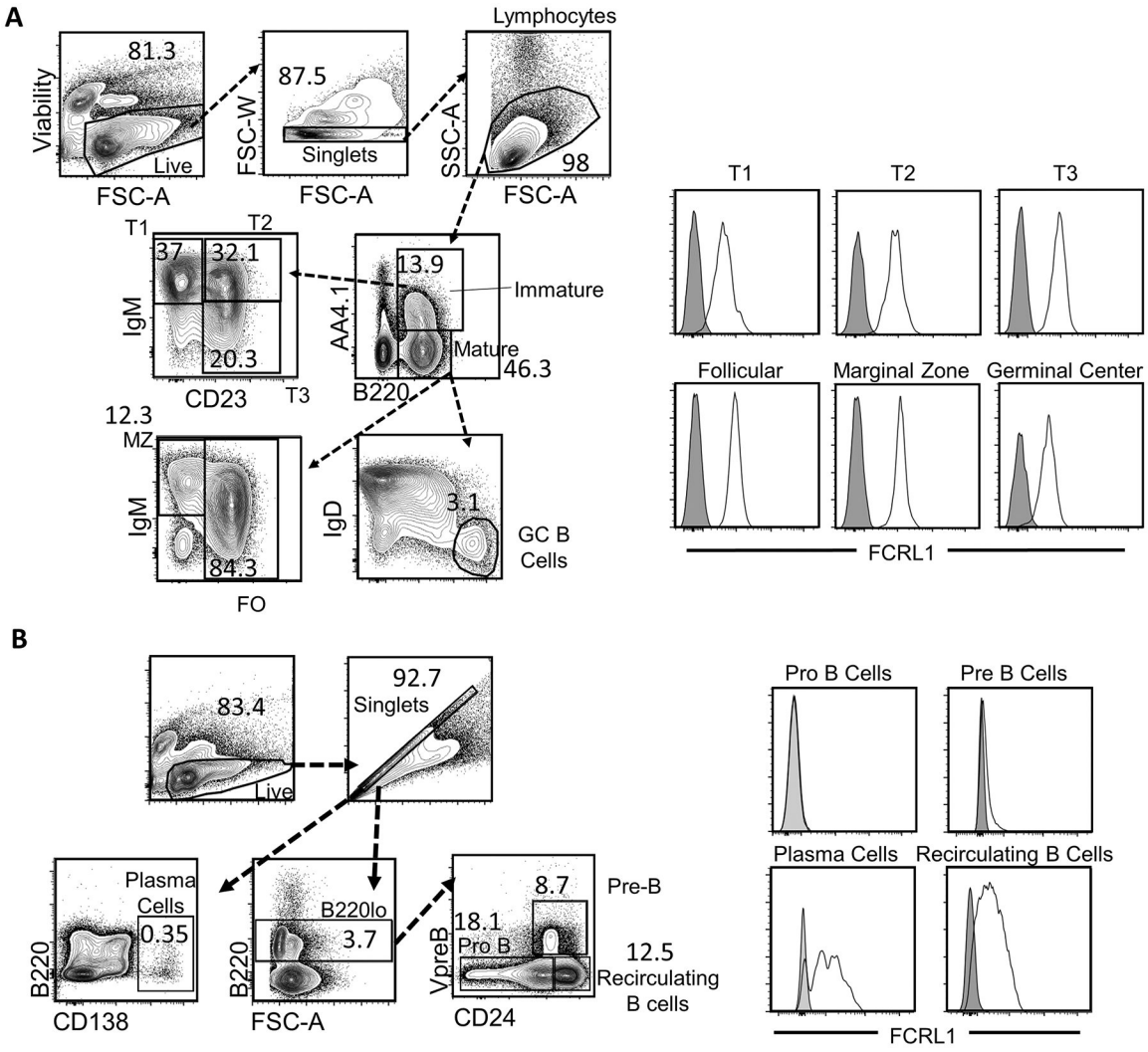

Figure 3. FCRL1 is expressed on mouse B cells beginning at the immature stage.

Flow cytometric measurement of mouse FCRL1 surface expression on B cells within a *(A)* splenocytes or *(B)* bone marrow. Gating strategies to identify key populations are shown to the left, with FCRL1 surface expression from WT 129/SvImJ (white peaks) and *Fcrl1*$^{-/-}$ (gray peaks) shown on histograms to the right. The plots shown are representative of at least 3 independent experiments.

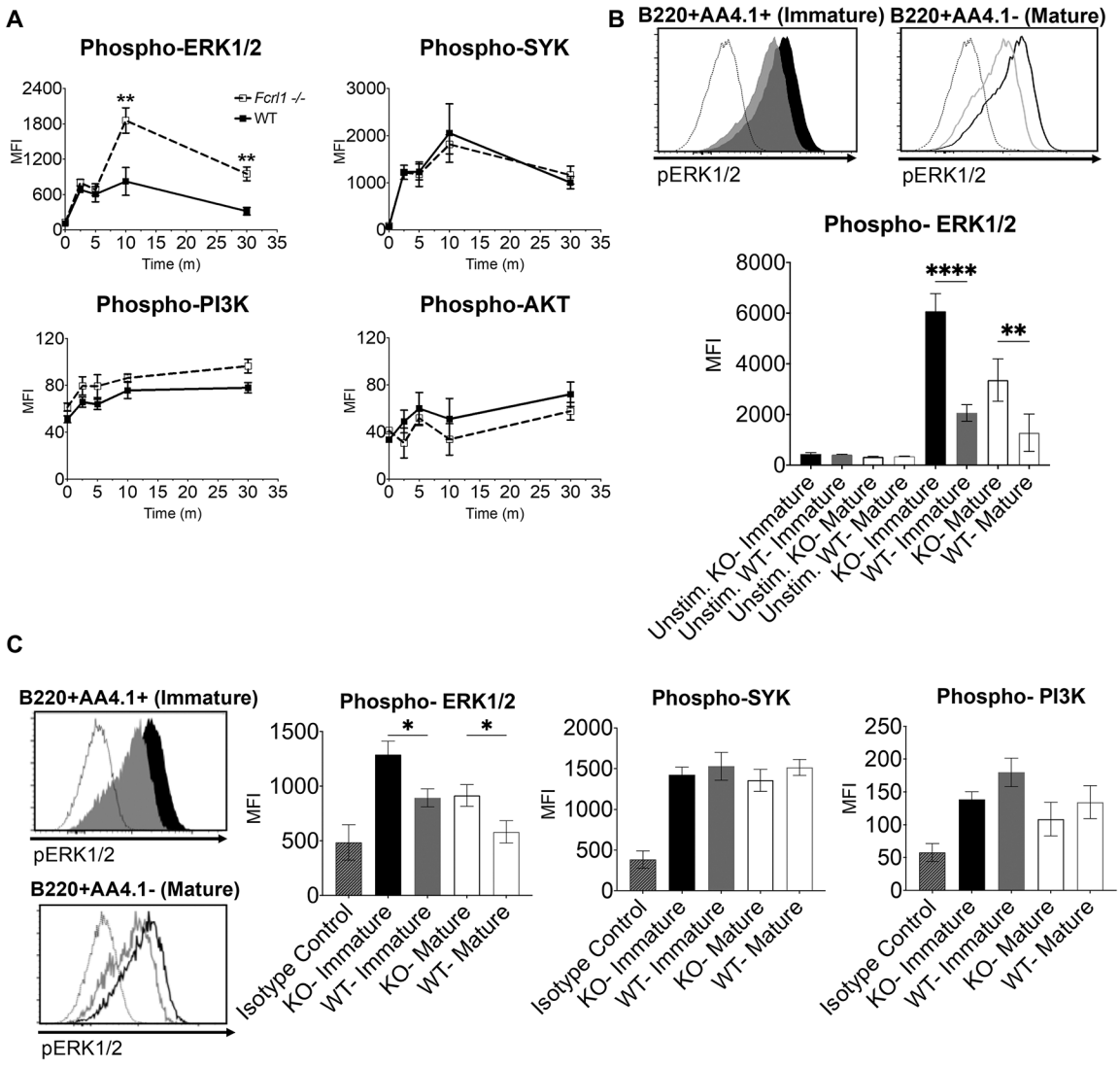

Figure 4. FCRL1 negatively regulates ERK phosphorylation in primary splenocytes.

*(A) F*low cytometric quantitation of ERK1/2, SYK, PI3K, and AKT phosphorylation after BCR crosslinking over time in WT (black line) and *Fcrl1*$^{-/-}$ (dashed line) isolated splenic B cells. *(B) Top,* Representative flow cytometry histograms of phospho-ERK1/2 in stimulated immature (B220^{+}AA4.1^{+}) and mature (B220^{+}AA4.1^{-}) splenic B cells including negative control of unstimulated cells (dotted line), *Fcrl1*$^{-/-}$ (black peak or line), and WT (gray peak or line). *Bottom,* Quantitation of replicate measurements of phospho-ERK in gated immature and mature B cells after polyclonal F(ab')$_2$ anti-Ig stimulation for 10 minutes. *(C)* Resting state ERK, SYK, and PI-3-K phosphorylation in mouse splenocytes disaggregated into fixative and gated on immature (B220^{+}AA4.1^{+}) and mature (B220^{+}AA4.1^{-}) B cells, with *Fcrl1*$^{-/-}$ (black peak or line), WT (gray peak or line), and isotype control (dotted line). *(B,C)* Data are representative of three independent experiments using n=3 age-matched female cohorts. Statistical tests of means were performed using one-way ANOVA with Tukey's test for post-hoc analysis. *p<0.05, **p<0.005.

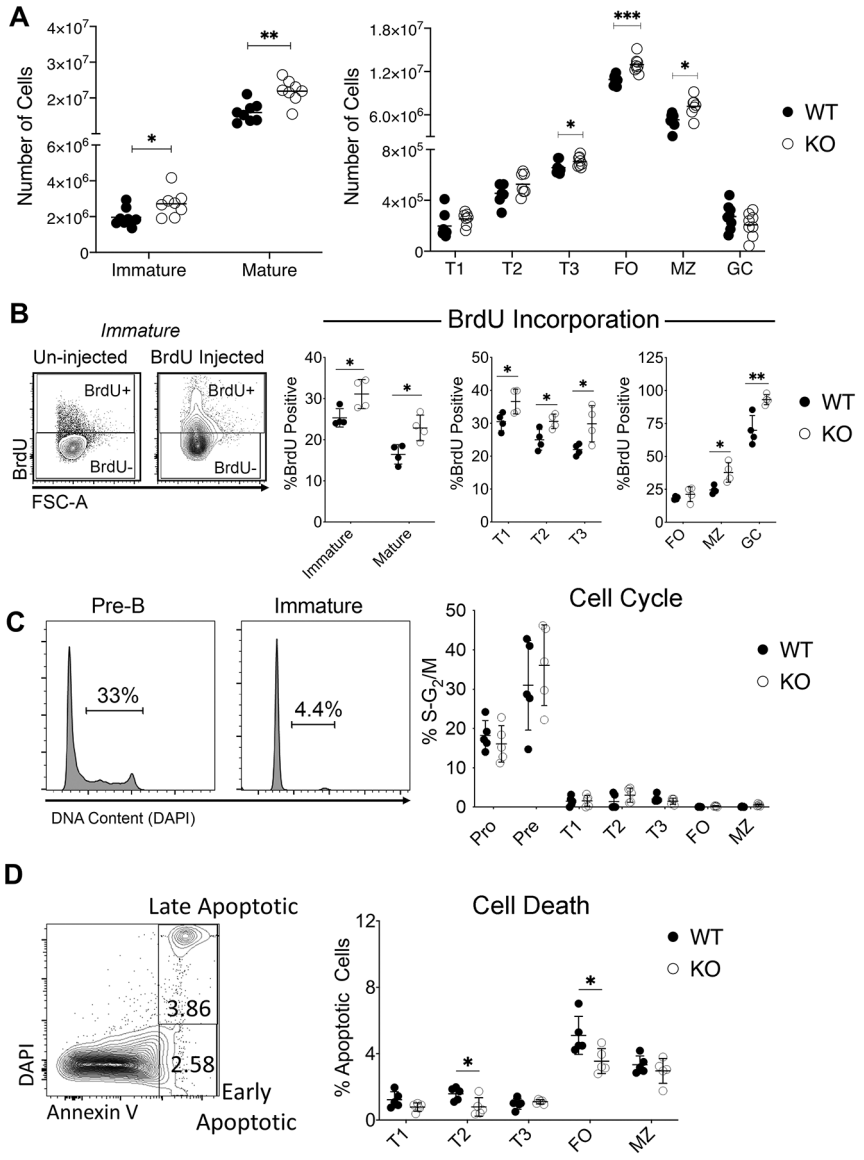

Figure 5. FCRL1 limits B cell numbers during maturation.

(A) Number of B cells in resting spleens enumerated by flow cytometry based on gating strategies shown in Figure 3. Splenic B cell numbers shown reflect gating on total immature ($B220^+AA4.1^+$) and total mature ($B220^+AA4.1^-$), T1 ($B220^+AA4.1^+IgM^{hi}CD23^-$), T2 ($B220^+AA4.1^+IgM^{hi}CD23^+$), T3 ($B220^+AA4.1^+IgM^{lo}CD23^+$), naïve follicular ($B220^+AA4.1^-CD23^+$), marginal zone ($B220^+AA4.1^-IgM^+CD23^-$), and germinal center ($B220^+AA4.1^+IgD^-GL7^+$) compartments of WT (black) and *Fcrl1*$^{-/-}$ (white) mice. Data are representative of 3 independent experiments on n=8 sex- and age-matched male and female cohorts. *(B)* Representative flow cytometric gating of immature B cells in control and BrdU-injected mice and quantitation of percentage of BrdU+ cells based on gating strategies shown in Figure 3. *(C)* Representative DAPI staining (left) for cell cycle analysis and quantitation of percent S/G2/M cells within of WT and *Fcrl1*$^{-/-}$ from bone marrow and splenic B cells. *(D)* Annexin V and propidium iodide staining to quantify apoptotic cells in

WT and *Fcrl1*$^{-/-}$ mice based on gating strategies shown in Figure 3. Data are representative of 3 independent experiments on n=4 age-matched female cohorts. Bars represent mean values. Two tailed student's T tests were used for statistical analysis: *p<0.05, **p<0.005, ***p<0.0005.